Journal of Industrial Microbiology & Biotechnology (2001) 26, 369–382

www.nature.com/jim

Convergent and divergent points in catabolic pathways involved in utilization of fluoranthene, naphthalene, anthracene, and phenanthrene by *Sphingomonas paucimobilis* var. EPA505

SP Story[1], SH Parker[2], SS Hayasaka[2], MB Riley[3] and EL Kline[2,4]

[1]*Environmental Biotechnology Section, Westinghouse Savannah River Company, Aiken, SC 29803;* [2]*Department of Microbiology, Clemson University, Clemson, SC 29634;* [3]*Department of Plant Pathology, Clemson University, Clemson, SC 29634;* [4]*Milkhaus South Laboratories Inc., Pendleton, SC 29650*

Catabolic pathways for utilization of naphthalene (NAP), anthracene (ANT), phenanthrene (PHE), and fluoranthene (FLA) by *Sphingomonas paucimobilis* EPA505 were identified. Accumulation of catabolic intermediates was investigated with three classes of Tn5 mutants with the following polycyclic aromatic hydrocarbon (PAH)-negative phenotypes; (class I NAP$^-$ PHE$^-$ FLA$^-$, class II NAP$^-$ PHE$^-$, and class III FLA$^-$). Class I mutant 200*pbhA* had a Tn5 insertion within a *meta* ring fission dioxygenase (*pbhA*), and a ferredoxin subunit gene (*pbhB*) resided directly downstream. Mutant 200*pbhA* and other class I mutants lost the ability to catalyze the initial dihydroxylation step and did not transform NAP, ANT, PHE, or FLA. Class I mutant 401 accumulated salicylic acid, 2-hydroxy-3-naphthoic acid, 1-hydroxy-2-naphthoic acid, and hydroxyacenaphthoic acid during incubation with NAP, ANT, PHE, or FLA, respectively. Class II mutant 132*pbhC* contained the Tn5 insertion in an aldolase hydratase (*pbhC*) and accumulated what appeared to be *meta* ring fission products: *trans*-*o*-hydroxybenzylidene pyruvate, *trans*-*o*-hydroxynaphylidene pyruvate, and *trans*-*o*-hydroxynaphthyl-oxobutenoic acid when incubated with NAP, ANT, and PHE, respectively. When mutant 132*pbhC* was incubated with 1-hydroxy-2-naphthoic acid, it accumulated *trans*-*o*-hydroxybenzylidene pyruvate. Class III mutant 104*ppdk* had a Tn5 insertion in a pyruvate phosphate dikinase gene that affected expression of a FLA-specific gene and accumulated a proposed *meta* ring fission product; *trans*-*o*-hydroxyacenaphyl-oxobutenoic acid during incubation with FLA. *Trans*-*o*-hydroxyacenaphyl-oxobutenoic acid was degraded to acenaphthenone that accumulated with class III mutant 611. Acenaphthenone was oxidized *via* incorporation of one molecule of dioxygen by another oxygenase. 2,3-Dihydroxybenzoic acid was the final FLA-derived catabolic intermediate detected. Analysis of PAH utilization mutants revealed that there are convergent and divergent points involved in NAP, ANT, PHE, and FLA utilization by *S. paucimobilis* EPA505. *Journal of Industrial Microbiology & Biotechnology* (2001) **26,** 369–382.

Keywords: *Sphingomonas*; mutants; fluoranthene; naphthalene; anthracene; phenanthrene

Introduction

Bacterial catabolic pathways for utilization of polycyclic aromatic hydrocarbons (PAHs) have been identified in naphthalene- and phenanthrene-degrading pseudomonads [3,6,21]. Use of recombinant bacteria carrying aromatic-degradative genes permitted identification of accumulated intermediate catabolites, yielded information on substrate specificity of enzymes, and allowed identification of PAH catabolic pathways [9,12,13,25]. The simplest PAH, naphthalene, consisting of two fused benzene rings, is relatively water-soluble, is degraded rapidly by microorganisms, and is used as a model compound for PAH biodegradation. Phenanthrene and fluoranthene consist of three and four fused rings, respectively. Two catabolic pathways have been proposed for phenanthrene utilization that diverges at 1-hydroxy-2-naphthoic acid [4,6,21]. Catabolic pathways for fluoranthene and other high molecular weight (HMW) PAHs have been proposed [2,14,18,19,22,24,32]; however, they are not as well defined as that of naphthalene and phenanthrene. Currently, there are two reports of the fluoranthene-degradative pathways used by *Mycobacterium* PYR-1 [18,19] and *Alcaligenes denitrificans* WWI [32] based on identification of ring fission and oxidation products and a comparison of the two pathways is given in a recent review on bacterial degradation of HMW PAHs [17].

Sphingomonads appear to have a great deal of catabolic versatility with respect to degradation of aromatic compounds [11,15,16,20,27]. During the degradation of naphthalene, phenanthrene, anthracene, and benz[*a*]anthracene by *Sphingomonas yanoikuyae* B1 (formerly named *Beijerinckia*), initial oxidation products catalyzed by a dioxygenase were identified and were the same as those reported for *Pseudomonas* species [16]. *S. yanoikuyae* B1 could also grow on a wide variety of monocyclic hydrocarbons and biphenyls. *S. aromaticivorans* F199, isolated from a subsurface formation rich in lignin-related compounds, has an extensive range in utilization of aromatic compounds [11]. Jackson *et al.* [15] proposed catabolic pathways for fluorene and fluoranthene by identification of catabolic intermediates by *Sphingomonas* sp. strain CO6, and from this information, inferred pathways used for catabolism of acenaphthene.

S. paucimobilis var. EPA505 was one of the first microorganisms reported to utilize fluoranthene as a sole carbon source [22]. Ten Tn5 mutant derivatives of strain EPA505 were isolated

Correspondence: Dr SP Story, Greengate Circle, Apartment 600J, Aiken, SC 29803, USA
Received 1 December 2000; accepted 26 April 2001

using Tn5 promoter probes and were grouped into three classes based on their loss of the ability to grow on naphthalene (NAP), phenanthrene (PHE), and/or fluoranthene (FLA) as a sole carbon source [31]. Class I mutants no longer grow on NAP, PHE, and FLA. A class II mutant that lost the ability to grow on NAP and PHE and the Tn5 insertion did not affect its growth on FLA. Class III mutants no longer grow on FLA and the Tn5 insertion did not affect their growth on NAP and PHE. Four of five mutants in class I lost the ability to convert indole to indigo, indicating loss of a specific hydroxylating dioxygenase function. One class I mutant and all class II and class III mutants retained the ability to convert indole to indigo. Based on DNA sequence analyses of regions flanking the Tn5 insert of one mutant from each class, PAH-degradative genes were identified or designated; class I 200*pbhA*, *pbhB* (Tn5 insertion within a *meta* ring fission dioxygenase gene, *pbhA*, with possible polar affect on expression of a ferredoxin subunit of a hydroxylating dioxygenase *pbhB*), class II 132*pbhC* (Tn5 insertion within a aldolase hydratase gene), class III 104*ppdk* (Tn5 insertion in a pyruvate phosphate dikinase gene *ppdk* with a possible polar effect on expression of a gene specific for FLA metabolism). The objectives of this study were to utilize the three classes of PAH utilization mutants of strain EPA505 to (1) identify intermediate catabolites during incubation with NAP, PHE, or FLA for delineation of the catabolic pathways, and (2) to propose other genes involved in PAH degradation by *S. paucimobilis* EPA505.

Materials and methods

Chemicals

Naphthalene, anthracene, phenanthrene, fluorene, fluoranthene, naphthalene d_{10}, phenanthrene d_{10}, fluorene d_{10}, fluoranthene d_{10}, salicylic acid, 1,2- and 2,3-hydroxynaphthoic acid, naphthenol, 9-fluorenone, 9-hydroxyfluorene, acenaphthol, 2,3- and 1,8-naphthalene dicarboxylic acid, hydroxyindane, 2,3- and 3,4-dihydroxybenzoic acid, and catechol (98–99% pure as determined by high-pressure liquid chromatography, HPLC), and bis(trimethylsilyl)-trifluoroacetamide were purchased from Aldrich (St. Louis, MO). HPLC and/or GC grade acetone, methanol, acetonitrile, ethyl acetate, phosphoric acid, and nanopure water were obtained from Fisher Scientific. Acenaphthenone was prepared from chemical oxidation of acenaphthenol [10]. Three oxidation products were identified (acenaphthenone, acenaphthquinone, and naphthalene anhydride) and acenaphthenone was purified using a solid phase extraction C_{18} cartridge [32]. Acenaphthenone purity was assessed by liquid and gas chromatography.

Organisms and growth conditions

The bacterial strain and mutants used are given in Table 1. The three classes of Tn5 mutants comprising 10 mutants defective in naphthalene (NAP), phenanthrene (PHE), and/or fluoranthene (FLA) metabolism were defined based on their inability to grow on one or more of these compounds as a sole carbon source [31].

Strain EPA505 was maintained on Luria–Bertani agar (LBA). Tn5 mutants were maintained on LBA with 50 μg ml^{-1} kanamycin (Km). For analyses of NAP-, ANT-, PHE-, or FLA-derived metabolites produced in culture medium by the wild type strain EPA505 or each of the Tn5 mutants, approximately 5×10^7 cells ml^{-1} (final concentration) was incubated at 28°C in 100 ml mineral salts medium (MSM) supplemented with 0.1 mg ml^{-1} each PAH and incubated for 5–72 h. At 5, 10, 24, 48, and 72 h, 100 ml of culture medium was extracted for analysis of PAH and

Table 1 Bacterial strain and mutants used in this study

Strain[a]	Promoter probe[b]	Relevant phenotype[c]
S. paucimobilis	EPA505	Fla$^+$, Phe$^+$, Ant$^+$, Nap$^+$, HNA$^+$, Sal$^+$, Cat$^+$, Indole$^+$, Col^r, Km^s, Tc^s
Class I mutants		
2[d]	*tc*$^-$	Indole$^-$, Fla$^-$, Phe$^-$, Nap$^-$, HNA$^+$, Sal$^+$, Cat$^+$, Col^r, Km^r
200[d,f] Tn5:*pbhA, pbhB*	*tc*^{induced}	Indole$^-$, Fla$^-$, Phe$^-$, Nap$^-$, HNA$^-$, Sal$^-$, Cat$^-$, Col^r, Km^r
300[d]	*tc*$^-$	Indole$^-$, Fla$^-$, Phe$^-$, Nap$^-$, HNA$^+$, Sal$^+$, Cat$^+$, Col^r, Km^r
394[e]	*lux*AB^{induced}	Indole$^-$, Fla$^-$, Phe$^-$, Nap$^-$, HNA$^-$, Sal$^-$, Cat$^-$, Col^r, Km^r
401[e]	*lux*AB$^-$	Indole$^+$, Fla$^-$, Phe$^-$, Nap$^-$, HNA$^-$, Sal$^-$, Cat$^+$, Col^r, Km^r
Class II mutant		
132[d,f] Tn5:*pbhC*	*tc*^{induced}	Indole$^+$, Fla$^+$, Phe$^-$, Nap$^-$, HNA$^-$, Sal$^+$, Cat$^+$, Col^r, Km^r
Class III mutants		
5[d]	*tc*$^-$	Indole$^+$, Fla$^-$, Phe$^+$, Nap$^+$, HNA$^+$, Sal$^+$, Cat$^+$, Col^r, Km^r
104[d,f] Tn5:*ppdk*	*tc*^{induced}	Indole$^+$, Fla$^-$, Phe$^+$, Nap$^+$, HNA$^+$, Sal$^+$, Cat$^+$, Col^r, Km^r
723[d]	*tc*$^-$	Indole$^+$, Fla$^-$, Phe$^+$, Nap$^+$, HNA$^+$, Sal$^+$, Cat$^+$, Col^r, Km^r
611[e]	*lux*AB$^-$	Indole$^+$, Fla$^-$, Phe$^+$, Nap$^+$, HNA$^+$, Sal$^+$, Cat$^+$, Col^r, Km^r

[a]Source of wild type strain EPA505 [22]; construction of Tn5 mutants, substrate utilization phenotype, and ability to convert indole to indigo [31].
[b]Mutants generated with the Tn5 encoded promoter probe in the correct orientation, *tc*^{induced}, or *lux*AB^{induced} or in the incorrect orientation, *tc*$^-$ or *lux*AB$^-$ [31].
[c]Abbreviations: Col, Tc, Km; colistin, tetracycline, and kanamycin; Fla, Phe, Nap, HNA, Sal, Cat; growth phenotype with naphthalene, anthracene, phenanthrene, fluoranthene, 1-hydroxy-2-naphthoic acid, salicylic acid, or catechol as a sole carbon source; (+) indicates growth, (−) indicates no growth.
[d]Mutants generated with Tn5 cassette encoding Km and promoterless *tc*.
[e]Mutants generated with Tn5 cassette encoding Km and promoterless *lux*AB.
[f]Genes that were previously identified flanking the Tn5 insert; *pbhA*, *meta* fission dioxygenase containing the Tn5 insertion; *pbhB*, ferrodoxin subunit directly downstream *pbhA*; *pbhC*, aldolase hydratase; *ppdk*, pyruvate phosphate dikinase (table modified from Story *et al.* [31]).

metabolites (described in Sections 2.3 and 2.4). MSM composition was described previously [31]. NAP, ANT, PHE, and FLA were prepared by dissolving 100 mg of each PAH in 1 ml acetone, which was filter-sterilized with a 0.2-μm pure size nylon filter (Fisher Scientific) prior to adding 100 μl PAH to MSM for a final amount at 0.1 mg PAH ml^{-1} MSM. All experiments were replicated at least four times.

Extraction of intermediate metabolites and PAH

Bacterial cells and excess PAH crystals were removed from PAH-amended MSM cultures by centrifugation at 1500×*g* for 30 min followed by filtration (0.45 μm nitrocellulose membrane; Whatman, Fisher Scientific, Pittsburgh, PA). Soluble PAH and intermediate catabolites from duplicate 100-ml culture filtrates were extracted and concentrated from culture medium either by passing culture filtrate through a C_{18} cartridge or partitioning it with 1:1 acidified ethyl acetate (pH 2.5). Metabolites were eluted from the C_{18} cartridge with 2 ml nonacidified solvent (acetone:methanol mixture, 3:2) followed by elution with 2 ml acidified (pH 2.5) acetone:methanol (3:2). Residual water in solvent extracts from solid phase extraction and partitioning was removed with anhydrous sodium sulfate (Fisher Scientific) and the solvent was then evaporated to dryness under a stream of N_2 gas. PAH and metabolites were redissolved in 1.0 ml acetone:methanol (3:2) for reverse-phase HPLC, or dissolved in 0.5 ml ethyl acetate for gas chromatography mass spectroscopy (GC-MS). Samples were derivatized for GC analyses by mixing them (1:1 v/v) with ethyl acetate and *N*-methyl bis trimethylsilyl trifluoracetamide (TMS) (Sigma Chemical, St. Louis, MO).

Analytical procedures

PAH and metabolites were analyzed by reverse-phase HPLC (Hewlett Packard 1090, Avondale, PA) equipped with a diode array detector and a C_{18} octadecylsilane column (10 cm×4.6 mm i.d., bead size 3 μm, pore size 100 Å; Regis Technologies, Morton Grove, IL). The HPLC solvent flow rate was 0.5 ml min^{-1}. The solvent system was acidic to facilitate better resolution of compounds and consisted of (A) 0.1% phosphoric acid in acetonitrile and (B) 0.1% phosphoric acid in 0.2% acetonitrile in nanopure water. The initial concentration of solvent B was 10% followed by a linear increase of 3% per minute to 92%. Wavelengths 214, 234, 254, 280, 325, and 350 nm were used for detection of specific PAHs and metabolites. Sample retention times and UV absorption spectra were compared to authentic standards (50 μg ml^{-1}) for identification of PAHs and intermediate catabolites.

A DB-5MS column (30 m length, 0.25 mm i.d., 0.25 μm film (J&W Scientific, Folsome, CA) was used for GC-MS analysis (Varian 3400, Saturn II system) with helium as the carrier gas. The column temperature program, injector temperature, and transfer line temperature were column temperature at 80°C for 2 min, followed by a linear increase of 8°C min^{-1} to 280°C for 4 min, injector temperature 270°C, and transfer line temperature 245°C. An ion trap mass spectrometer was set for a scan monitoring mode from 45 to 550 amu. Total ion chromatograms and mass spectra were analyzed utilizing Saturn software (Varian Instruments, Pala Alto, CA) system software. Mass spectra of deuterated and non-deuterated PAHs and intermediate metabolites were analyzed according to the fragmentation rules established for PAH-derived intermediate metabolites derivatized with trimethylsilyl reagent [33]. Sample GC retention times and mass spectra were compared to authentic standards (20 μg ml^{-1}) for identification of PAHs and intermediate catabolites.

Direct probe mass spectroscopy (Thermabeam, Extrel) was performed with samples purified by HPLC (Hewlett Packard 1090) that were dried under a stream of N_2 gas and dissolved in 1:1 acetonitrile:water. The sample passed through a nebulizer directly to a quadrupole mass spectrometer (current at 1 mA, 1000 V; argon pressure at 810 Torr; LC flow rate at 1.0 ml min^{-1}; nebulizer temperature tip at 230°C, backend 110°C). Total ion chromatograms and mass spectra were recorded using the Ionization™ ABB-Extrel system software.

Results

The bacterial strains used in this study are described in Table 1. Reverse-phase HPLC and GC-MS were used to analyze catabolic intermediates produced by the wild type or accumulated by mutants during incubation with naphthalene (NAP), anthracene (ANT), phenanthrene (PHE), or fluoranthene (FLA), and the deuterated forms of NAP, PHE, or FLA. Accumulation of compounds by mutants was indicated by an increase in the HPLC peak area as compared to the same compound detected with the wild type that had the same HPLC retention time and UV absorption spectrum (Table 2 and Figure 1). PAH and catabolites were extracted from culture filtrates at 5, 10, 24, 48, and 72 h. Maximum accumulation of catabolic products with mutants was achieved within 72 h during incubation with a specific PAH. The UV absorption spectra in Figure 1 were recorded at pH 2.5. Compounds were purified by HPLC and derivatized with trimethylsilyl reagent (TMS, mass 73) by GC-MS. The use of deuterated PAHs (NAPd_8, PHEd_{10}, and FLAd_{10}) verified that the TMS-derivatized compounds detected by GC-MS were PAH-derived catabolites.

Class I mutants defective in naphthalene, anthracene, phenanthrene, and fluoranthene metabolism

Four class I mutants, two 200Tn5:*pbhA*, 300, and 394 appeared to be completely impaired in PAH transformation. HPLC and GC-MS analyses did not detect any PAH-derived catabolites in culture filtrates of these mutants incubated with NAP, ANT, PHE, or FLA. However, the indole-positive class I mutant 401 accumulated hydroxyaromatic acids when incubated with these PAHs.

Accumulation of naphthalene, anthracene, and phenanthrene ring fission products by a class II mutant

Class II mutant 132Tn5:*pbhC* accumulated a yellow compound (at pH7) after 72 h incubation with naphthalene (NAP) having an HPLC retention time (RT) of 11.7 min (Table 2) and UV absorption spectrum shown in Figure 1B. GC-MS analysis detected three compounds with retention times of 16.1, 16.3, and 16.4 min. The mass spectra (MS) of these compounds were consistent with that of *trans*-*o*-hydroxybenzylidene pyruvate derivatized at three, two, or one position(s) with TMS-derivatizing reagent. The compound with a GC RT of 16.3 min occurred in the greatest abundance and had a M+ at m/z 336 and major fragment

Table 2 HPLC retention times of PAH-derived compounds detected by HPLC with *S. paucimobilis* EPA505 and Tn5 induced PAH mutants after incubation with naphthalene, anthracene, phenanthrene, or fluoranthene

Compound/strain	Incubation time (h)	HPLC retention time (min, λ[a])	HPLC peak area (amu/s)	Identity[b]
Naphthalene/Tn5 mutants				
Class II 132 Tn5:*pbhC*	72	11.7, 325	25,252	ring fission naphthalene[c]
Class I 401 PbhE	72	10.4, 234	37,292	salicylic acid
EPA505	5	11.7, 325	953	ring fission naphthalene[c]
	24	10.4, 234	13,725	salicylic acid
	48	10.4, 234	11,492	salicylic acid
	72	ND[d]	ND	ND
1-Hydroxy-2-naphthoic acid/Tn5 mutant				
Class II 132 Tn5:*pbhC*	72	11.7, 325	19,474	ring fission naphthalene[c]
Anthracene/Tn5 mutants				
Class II 132 Tn5:*pbhC*	72	12.8, 254	20,327	ring fission anthracene[c]
Class I 401 PbhE	72	16.1, 254	16,014	2-hydroxy-3-naphthoate
EPA505	5	16.1, 254	8,736	2-hydroxy-3-naphthoate
	24	16.1, 254	1,093	2-hydroxy-3-naphthoate
	48	11.7, 325	4,026	ring fission NAP[c]
	72	6.2, 214	3,256	catechol
Phenanthrene/Tn5 mutants				
Class II 132 Tn5:*pbhC*	72	17.6, 254	32,805	ring fission phenanthrene[c]
Class I 401 PbhE	72	16.4, 254	26,372	1-hydroxy-2-naphthoate
EPA505	5	17.6, 254	6,434	ring fission phenanthrene[c]
	24	16.4, 254	6,598	1-hydroxy-2-naphthoate
	48	16.4, 254	2,390	1-hydroxy-2-naphthoate
	72	ND	ND	ND
Fluoranthene/Tn5 mutants				
Class III 104 Tn5:*ppdk*	72	15.4, 350	26,622	ring fission fluoranthene[c]
Class I 401 PbhE	72	14.1, 234	19,528	hydroxyacenaphthoate[c]
Class III 611 PbhF	72	16.2, 254	20,906	acenaphthenone
Class III 611 PbhF		12.6, 234	4,896	hydroxymethylbenzocoumarine[e]
Class III 611 PbhF		14.4, 254	2,412	1,8-naphthalene-dicarboxylic acid[f]
EPA505	5	15.4, 350	985	ring fission fluoranthene[c]
	24	15.4, 350	1,430	ring fission fluoranthene[c]
	48	16.2, 254	5,404	acenaphthenone
	72	12.6, 234	7,939	hydroxymethylbenzocoumarine[e]
	72	7.2, 214	1,729	2,3-dihydroxybenzoate

[a]Wavelength (nm) used for detection.
[b]Identity determined by comparing HPLC and UV absorption spectrum of the sample to that of a standard. UV absorption spectra were reported at pH 2.5 (see).Figure 1
[c]If standards were not available, then identity was proposed based on UV absorption spectra and mass spectra.
[d]ND, either compound was not detected or identity was not determined by HPLC analysis.
[e]Identification based on UV absorption spectrum reported by Weissenfels *et al.* [32].
[f]1,8-Naphthalene-dicarboxylic acid identified by HPLC was detected as naphthalene anhydride with GC-MS analysis (Table 3). For the wild type, several HPLC peaks were observed and only the compound with the greatest peak area is given for that incubation period. The peak areas for compounds detected with mutants are an average of three replicates.

ions 219 (loss of COO-TMS) and 73 (TMS) (Figure 2A). When incubated with NAPd_8, a deuterated NAP ring fission product was identified, verifying that this was a NAP-derived catabolite. A shift of 6 amu was observed as compared to the nondeuterated form (Figure 2A, the numbers in brackets for major ionization fragments are given for the deuterated ions). When mutant 132Tn5:*pbhC* was incubated with 1-hydroxy-2-naphthoic acid, it accumulated a compound that had identical HPLC and GC-MS characteristics to the compound that accumulated when this mutant was incubated with NAP (Table 2, Figure 2A).

When incubated with PHE, 132Tn5:*pbhC* accumulated a yellow compound (pH 7) having an HPLC RT of 17.6 min (Table 2) and the UV absorption spectrum shown in Figure 1E. GC-MS analysis detected two compounds at GC RT of 23.1 and 24.8 as TMS derivatives. The mass spectrum of the compound at 24.8 min had a M+ at m/z 386 and ionization fragments 371 (loss of CH_3, contributed by TMS), 269 (loss of COO-TMS), and 73 (TMS) (Figure 2B). TMS at three positions on the open ring of PHE (GC RT=23.1 min) was also detected (Table 3). When incubated with PHEd_{10}, a deuterated form accumulated with a GC RT of 23.2 min, and the mass spectrum had a shift of 8 amu for major ionization fragments (Figure 2B, numbers in brackets). The molecular weight and fragmentation pattern of this compound indicate a ring fission product of PHE degradation. During incubation with anthracene (ANT) this, mutant accumulated a compound that had a similar HPLC RT to the PHE-derived catabolite (Table 2); however, the UV absorption spectrum was considerably different (Figure 1H, ANT catabolite; Figure 1E, PHE catabolite). The mass spectrum of

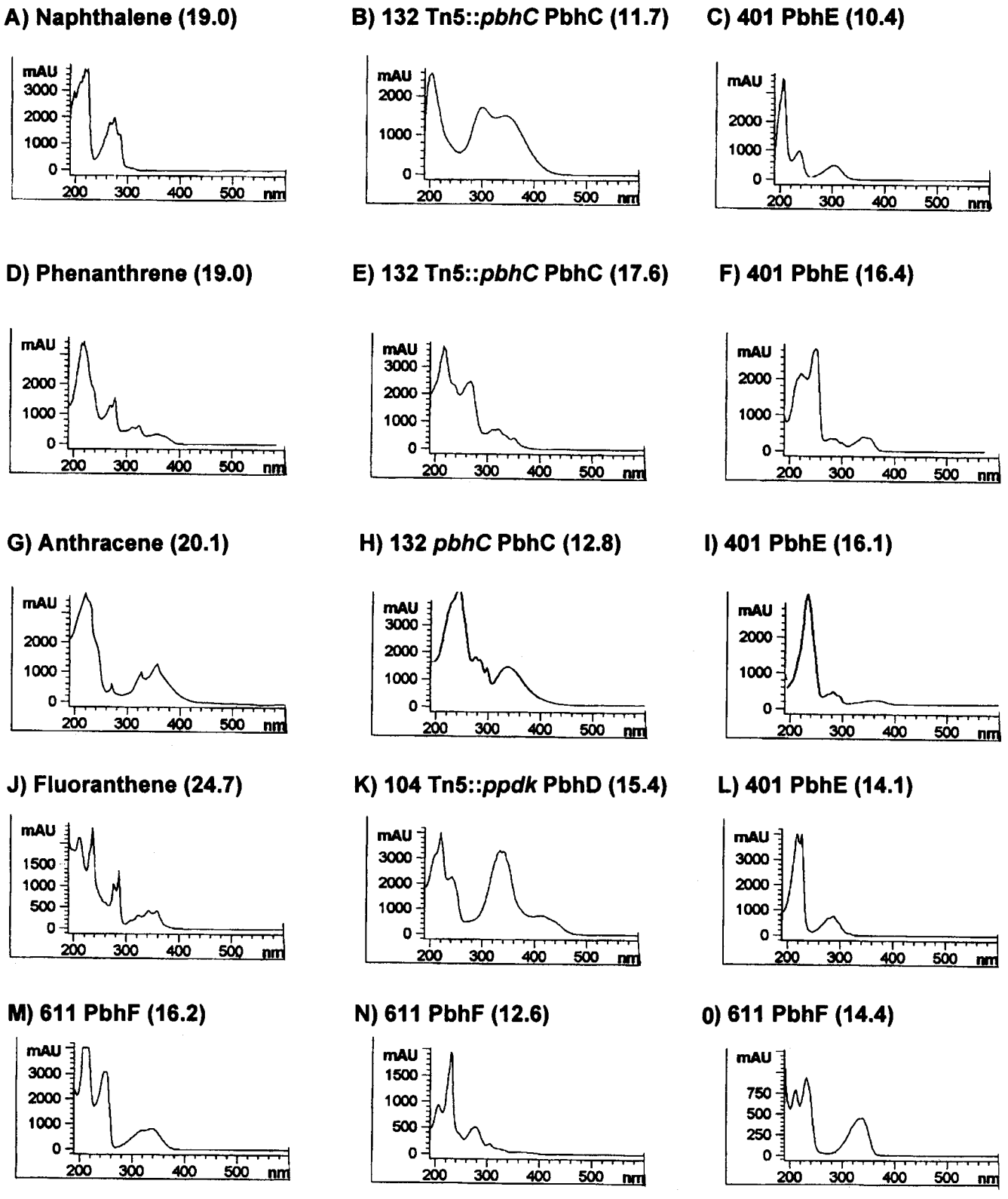

Figure 1 UV absorption spectra of parent PAHs and metabolites detected by HPLC in culture supernatants of bacteria incubated with (A) naphthalene, (D) phenanthrene, (G) anthracene, or (J) fluoranthene. HPLC retention time in minutes is given for the compound detected following mutant designation. Catabolites accumulated with mutants: (B) naphthalene ring fission, (C) salicylic acid, (E) phenanthrene ring fission, (F) 1-hydroxy-2-naphthoic acid, (H) anthracene ring fission, (I) 2-hydroxy-3-naphthoic acid, (K) fluoranthene ring fission, (L) hydroxyacenaphthoic acid, (M) acenaphthenone. Other compounds detected with mutant 611 PbhF: (N) hydroxymethylbenzocoumarine, (O) 1,8-naphthalene dicarboxylic acid. For catabolites shown in figures (C), (F), (I), (M), and (O), the HPLC retention time and UV absorption spectra matched that of standards used. UV absorption spectra were determined at pH 2.

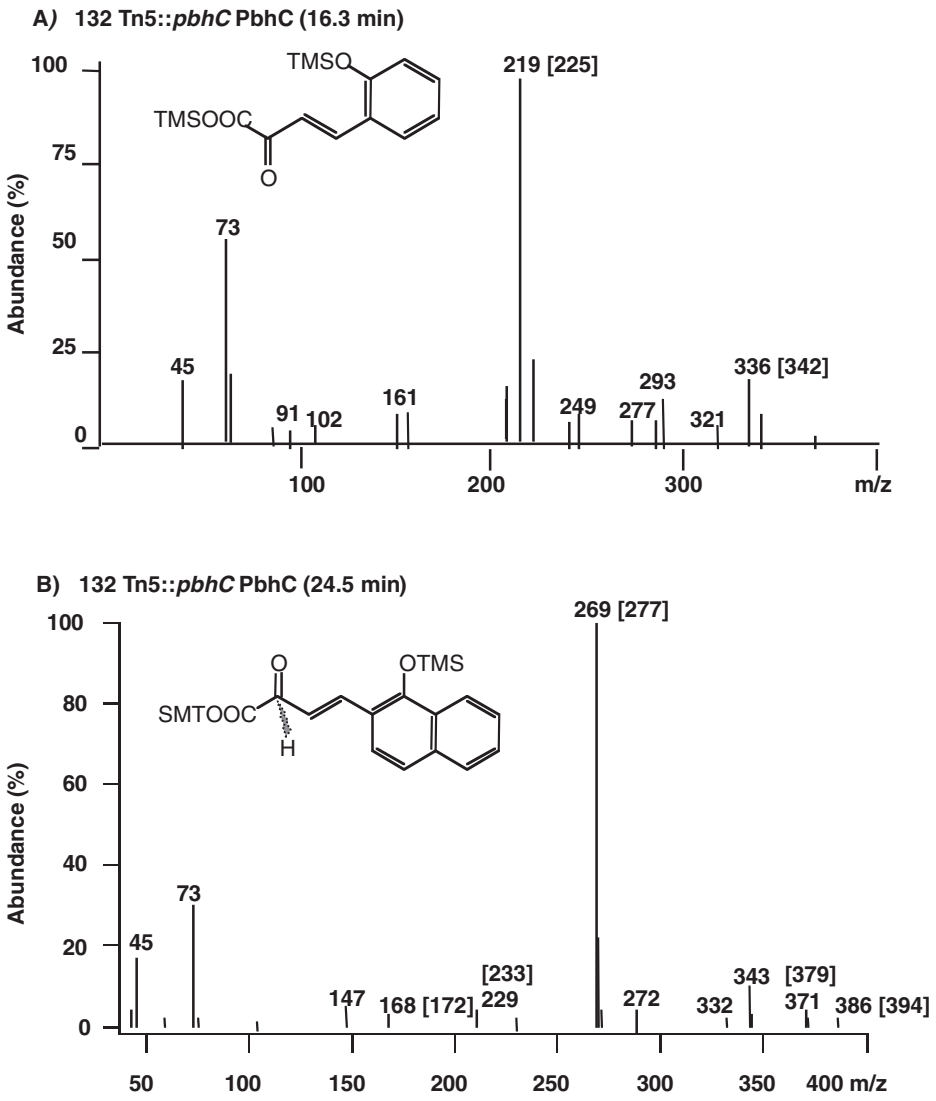

Figure 2 Mass spectra of trimethylsilyl-derivatized (AMU 73) ring fission products accumulated by mutant 132 Tn5:*pbhC* PbhC when incubated with (A) naphthalene or naphthalene d_8 and (B) phenanthrene or phenanthrene d_{10}. Gas chromatography retention time is given following mutant designation. Deuterated fragments are given in brackets.

the ANT-derived catabolite was almost identical to that observed in Figure 2B (Table 3).

Identification of naphthalene-, anthracene-, phenanthrene-, and fluoranthene-derived catabolic products accumulated by a class I mutant

When incubated with NAP, class I mutant 401 accumulated a colorless compound having an HPLC RT of 10.4 min (Table 2) and UV absorption spectrum matching salicylic acid (Figure 1C). GC-MS analysis confirmed the identity by showing an identical GC RT of 13.2 min and M+ at m/z 282 with major fragment ions 267 (loss of CH_3 contributed by TMS) and 73 (TMS) (Figure 3A) as the standard. A shift of 4 amu for deuterated salicylic acid was observed when this mutant was incubated with NAPd_8 (Figure 3A, numbers in brackets).

Class I mutant 401 accumulated a colorless compound when incubated with PHE that was identical to the HPLC RT (16.4 min) (Table 2) and UV absorption spectrum of 1-hydroxy-2-naphthoic acid (1,2-HNA) (Figure 1F). GC-MS confirmed the identity of 1,2-HNA showing a GC RT of 20.1 min with M+ at m/z 332 and fragmentation ions 317 (loss of CH_3), 244 (loss of TMSO), and 73 (TMS) compared to the TMS-derivatized 1,2-HNA standard (Figure 3B). The deuterated form is also given (Figure 3B, numbers in brackets).

During incubation with ANT, mutant 401 accumulated a colorless compound (Table 2) with an identical HPLC RT and UV absorption spectrum to 2-hydroxy-3-naphthoic acid (Figure 1I). 2-Hydroxy-3-naphthoic acid had an identical GC RT and mass spectrum as that observed for 1-hydroxy-2-naphthoic acid (Figure 3B).

Since mutants 132Tn5:*pbhC* and 401 accumulated different catabolic intermediates, where the Tn5 specifically affected NAP and PHE utilization in the former and NAP, ANT, PHE, and FLA utilization was lost in the latter, the PAH-negative phenotype of mutant 401 was designated PbhE.

When mutant 401 was incubated with FLA, it accumulated a compound with an HPLC RT of 14.1 min (Table 2) with the UV

Table 3 GC mass spectral analyses of PAH-derived metabolites and deuterated forms found with the wild type or Tn5 mutants

Identity	RT (min)[a]	M^{+}[b]	Ionization fragments[c]
Naphthalene[d]	*7.5*	*128 (100)*	*102(10), 87, 75, 63, 51*
Naphthalened$_8$[d]	*7.7*	*136 (100)*	*109, 64*
Dihydroxynaphthalene[d,e]	16.5	304 (100)	299, 269, 227, 215 (17), 185, 145 (10), 129, 117, 95, 73 (40), 45
Ring fission NAP (1× TMS)[e,f]	16.4	263 (5)	248 (35), 220, 175 (100), 147 (65), 161, 103 (22), 91 (10), 73 (11)
Ring fission NAP (3× TMS)[e,f]	16.1	411 (8)	395, 323 (20), 296 (40), 221 (100), 179 (20), 163 (15), 147, 103, 73 (21)
Catechol[d,e]	11.2	254 (59)	239 (100), 223 (10), 209, 179, 147, 133, 112 (10), 91, 73 (28)
Anthracene[d]	*17.5*	*178 (100)*	*152, 126, 76*
Ring fission ANT (2× TMS)[e,f]	23.9	386 (2)	371, 343 (10), 297, 269 (100), 253, 211, 168, 147, 73 (58), 45 (17)
2-Hydroxy-3-naphthoic acid[d,e,f]	20.2	332 (1)	318 (22), 317 (100), 260, 244, 185, 147, 114, 87, 73 (32), 45 (12)
Phenanthrene[d]	*17.2*	*178 (100)*	*152 (18), 126, 89, 76, 63, 40*
Phenanthrene d_{10}[d]	*17.4*	*188 (100)*	*156, 128, 112, 80, 52, 42*
Dihydroxyphenanthrene[d,e]	23.3	354 (100)	339, 280, 266 (10), 264, 147, 113, 87, 73 (39), 57, 43 (10)
Dihydroxyphenanthrene d_8[d,e]	23.4	362 (79)	361 (30), 347 (30), 280, 274 (20), 187, 158, 73 (25), 59, 45, 43
Ring fission PHE (3× TMS)[e,f]	23.1	460 (4)	445 (11), 417, 371, 343 (100), 269, 253 (10), 205, 181, 147, 73 (32), 45
Ring fission PHEd_8 (3× TMS)[e,f]	23.2	468 (1)	453, 351 (100), 335, 260 (12), 244, 189, 147, 73 (33), 45
1-Hydroxy-2-naphthoic acid[d,e,f]	21.0	332/333 (1)	320 (10), 319 (22), 317 (100), 185 (10), 147 (8), 87, 73 (32), 55, 45
Salicylic acid[d,e,f]	13.2	283/282 (2)	270, 269 (25), 267/268 (100), 210, 149 (11), 135 (15), 73 (62), 45 (20)
Fluoranthene[d]	*21.5*	*202 (100)*	*150, 101, 88, 74, 62, 50*
Fluoranthene d_{10}[d]	*21.8*	*212 (100)*	*156, 106 (21), 92 (15), 64 (12)*
Dihydroxyfluoranthene[e]	27.3	378 (100)	304, 290 (38), 274, 260 (11), 230, 215, 189, 149, 73, 45
Dihydroxyfluoranthene d_8[e]	27.3	386 (85)	371, 298 (30), 268, 223, 208, 195, 146, 119, 85, 73 (100), 57
Acenaphthenol[d,e,f]	18.1	241 (30)	240 (100), 225, 197 (13), 165 (22), 139 (20), 113, 89, 73 (45)
Acenaphthquinone[e]	19.2	182 (58)	154 (100), 141, 126 (80), 98, 87 (10), 74, 63, 50 (11), 41
Acenaphthquinone d_6[e]	19.3	188 (40)	160 (98), 132 (100), 147, 100, 101, 102, 79 (12), 75 (18), 65, 52 (18)
Naphthalene anhydride[d,e]	20.6	198 (45)	193, 181, 163, 154 (100), 145, 126 (65), 115, 100, 87, 74, 63, 50
Naphthalene anhydride d_6[e]	20.7	204 (48)	162 (32), 160 (100), 147, 132 (78), 101, 90, 76 (12), 65 (10), 52, 42
2,3-Dihydroxy-benzoic acid[d,e]	15.5	371 (2)	356 (100), 355 (58), 281 (20), 267, 221 (17), 133, 73 (98), 59, 45 (12)
Fluorene[d]	*14.4*	*166 (100)*	*139 (10), 115, 83 (22), 63 (10), 50 (10), 39*
Fluorene d_{10}[d]	*14.5*	*176 (100)*	*149, 87 (15)*
Hydroxyindane[d,e]	13.6	205 (20)	204 (98), 189 (15), 145, 131, 115 (30), 103 (18), 73 (100), 45 (30)
Hydroxyindane d_7[e]	13.9	211 (22)	208 (82), 193 (15), 137 (33), 119 (25), 109 (15), 73 (100), 5 8, 45 (28)
Indanone[e]	8.3	132 (39)	104 (100), 92 (11), 77 (15), 51
Indanone d_7[e]	8.4	137 (29)	108 (100), 81 (30), 52 (15)

[a]Gas chromatography retention time.
[b]M^{+} = Molecular ion.
[c]Major ionization fragments are given with ≥10% threshold value; percent abundance of major ionization fragments is represented in parentheses.
[d]Parent PAH or standards used in this study.
[e]Catabolites found with the wild type; 1,8-naphthalene-dicarboxylic acid was detected as naphthalene anhydride.
[f]Compounds accumulated by mutants and proposed ring fission products derivatized with TMS at one, two, or three positions were found either with the wild type or mutant strain that are not given in Figures 2–4.

absorption spectrum shown in Figure 1L. The GC RT was 24.1 min and the mass spectrum had a M+ at *m/z* 357, and major ionization fragments at *m/z* 239 (loss of COOTMS from M+) and 73 (TMS) (Figure 3C). Based on this GC RT and fragmentation pattern, we propose this compound to be hydroxyacenaphthoic acid.

Accumulation of fluoranthene-derived catabolic products by class III mutants

Class III mutants, 5, 104Tn5:*ppdk*, and 723 accumulated a red (pH 7) compound when incubated with fluoranthene (FLA) that had an HPLC RT of 15.4 min (Table 2) and UV absorption spectrum given in Figure 1K. The UV absorption spectrum was recorded at pH 2.5 (Figure 1K) and this compound appears yellow at this pH. This red compound only transiently appeared with the class III mutant 611. Mutant 104Tn5:*ppdk* accumulated the highest levels of this compound and was chosen for further analyses.

GC-MS analysis of extracts of culture supernates containing the red color or HPLC-purified fractions of the red compound revealed that the compound had a GC RT of 30.6 min that had a M+ at *m/z* 411 and major ionization fragments at *m/z* 395 (loss of CH_3), 321 (loss of OTMS from M+), 294 (loss of COOTMS from M+), 192 (loss of OTMS from fragment at *m/z* 280), and 73 (TMS) (Figure 4A, deuterated fragments in brackets). Direct probe mass spectral analysis on pooled fractions from HPLC purification of the non-TMS-derivatized red compound revealed a M+ at *m/z* 267 and major ionization fragments at *m/z* 221 (loss of COOH from M+), 192 (loss of CHO from AMU 221), 180 (loss of CH from AMU 192), 168 (loss of CH from AMU 180), 152 (loss of CO from AMU 180), and 139 (loss of CO from AMU 168). Based on the fragmentation pattern of both the derivatized (GC-MS) and nonderivatized compound (direct probe MS), a *meta* ring fission product of FLA catabolism is proposed. This phenotype of mutant 104 resulting from the Tn5 insertion in *ppdk* is designated PbhD.

When the class III mutant 611 was incubated with FLA, a colorless compound from the nonacidified fraction of the culture supernate was detected by HPLC with the same retention time (16.2 min) and UV absorption spectrum as acenaphthenone that was detected with the wild type (Table 2, Figure 1M). The acidified fraction was black and two compounds were detected in this

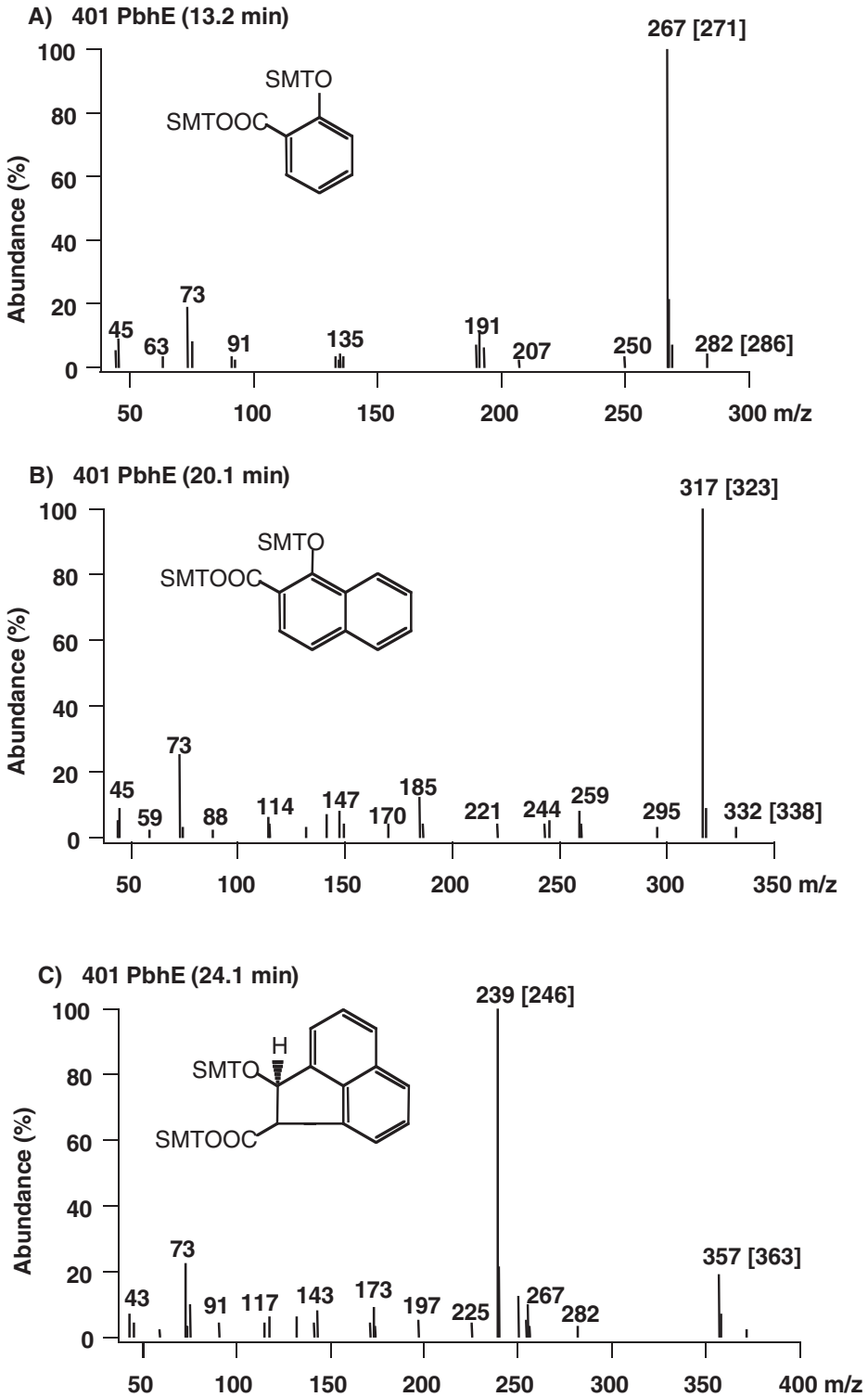

Figure 3 Mass spectra of trimethylsilyl-derivatized (AMU 73) ring fission products accumulated by mutant 401 PbhE when incubated with (A) naphthalene or naphthalene d_8, (B) phenanthrene or phenanthrene d_{10}, and (C) fluoranthene or fluoranthene d_{10}. Gas chromatography retention time is given following mutant designation. Deuterated fragments are given in brackets.

fraction that had an HPLC RT of 12.6 and 14.4 min. (Table 2). The compound at 12.6 min was the black compound and had an UV absorption spectrum identical to hydroxymethylbenzocoumarine (HMBC) [32] identified during analysis of fluoranthene catabolic intermediates of *A. denitrificans* WWI. (Figure 1N). The other compound (HPLC RT 14.4 min) was colorless and had an HPLC RT and UV absorption spectrum identical to that of 1,8-naphthalene-dicarboxylic acid (1,8-NDC) (Figure 1). GC analysis detected acenaphthenone as a major accumulated product by mutant 611 with a retention time of 15.5 min. The mass spectrum of

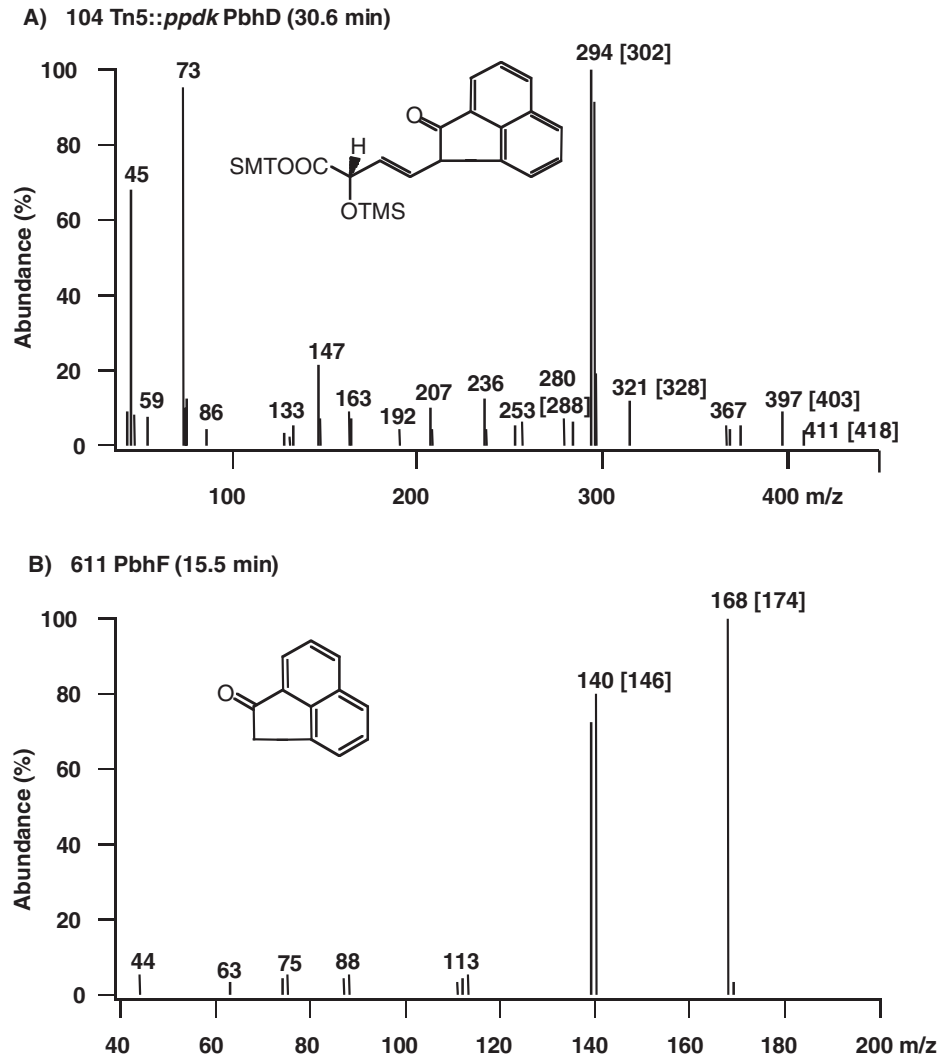

Figure 4 Mass spectra of trimethylsilyl-derivatized (AMU 73) ring fission products accumulated by (A) mutant 104 Tn5:*ppdk* PbhD or (B) mutant 611 PbhF when incubated with fluoranthene or fluoranthene d_{10}. Gas chromatography retention time is given following mutant designation. Deuterated fragments are given in brackets.

acenaphthenone showed a M+ at m/z 168 and major fragment ion of m/z 140 (loss of CO) (Figure 4B). The TMS-derivatized acenaphthol was also identified by GC-MS (Table 3). This particular FLA utilization phenotype disrupted in mutant 611 was designated PbhF. The putative HMBC detected by HPLC in culture extracts of mutant 611 was not detected during GC analysis. HMBC was previously reported to be thermally unstable and therefore not amenable to GC analysis [32]. 1,8-NDC was detected as naphthalene anhydride during GC analysis. Mutant 611 incubated with FLAd_{10} accumulated acenaphthenone d_6 having a similar GC retention time as the nondeuterated form (Figure 4B, numbers in brackets).

Detection of intermediate metabolites formed by wild type strain EPA505 growing on naphthalene, anthracene, phenanthrene, and fluoranthene

Wild type EPA505 produced a transient appearance of intermediate metabolites over 72 h when grown on NAP, ANT, PHE, or FLA (Table 2). Hydroxy aromatic acids were the primary catabolites detected when the wild type was incubated with NAP, ANT, or PHE. The dihydroxylated forms of NAP and PHE were consistently identified by GC-MS and catechol was the final catabolite detected during utilization of these PAHs (Table 3). Dihydroxynaphthalene d_6 and dihydroxyphenanthrene d_8 were also detected (Table 3).

During growth of EPA505 on FLA, three intermediate metabolites were detected by HPLC (Table 2). Metabolite 1 had a HPLC retention time of 15.4 min and a UV absorption spectrum, which did not match any of the standards used and was identical to the catabolic intermediate accumulated by mutant 104Tn5:*ppdk* (Table 2, Figure 1K). The second metabolite had an HPLC retention time and UV absorption spectrum that was identical to acenaphthenone, which accumulated with mutant 611 (Table 2, Figure 1M). A third metabolite appeared after acenaphthenone and had a HPLC retention time and a UV absorption spectrum that was identical to that of 3-hydroxymethyl-4,5-benzocoumarine (Table 2, Figure 1N).

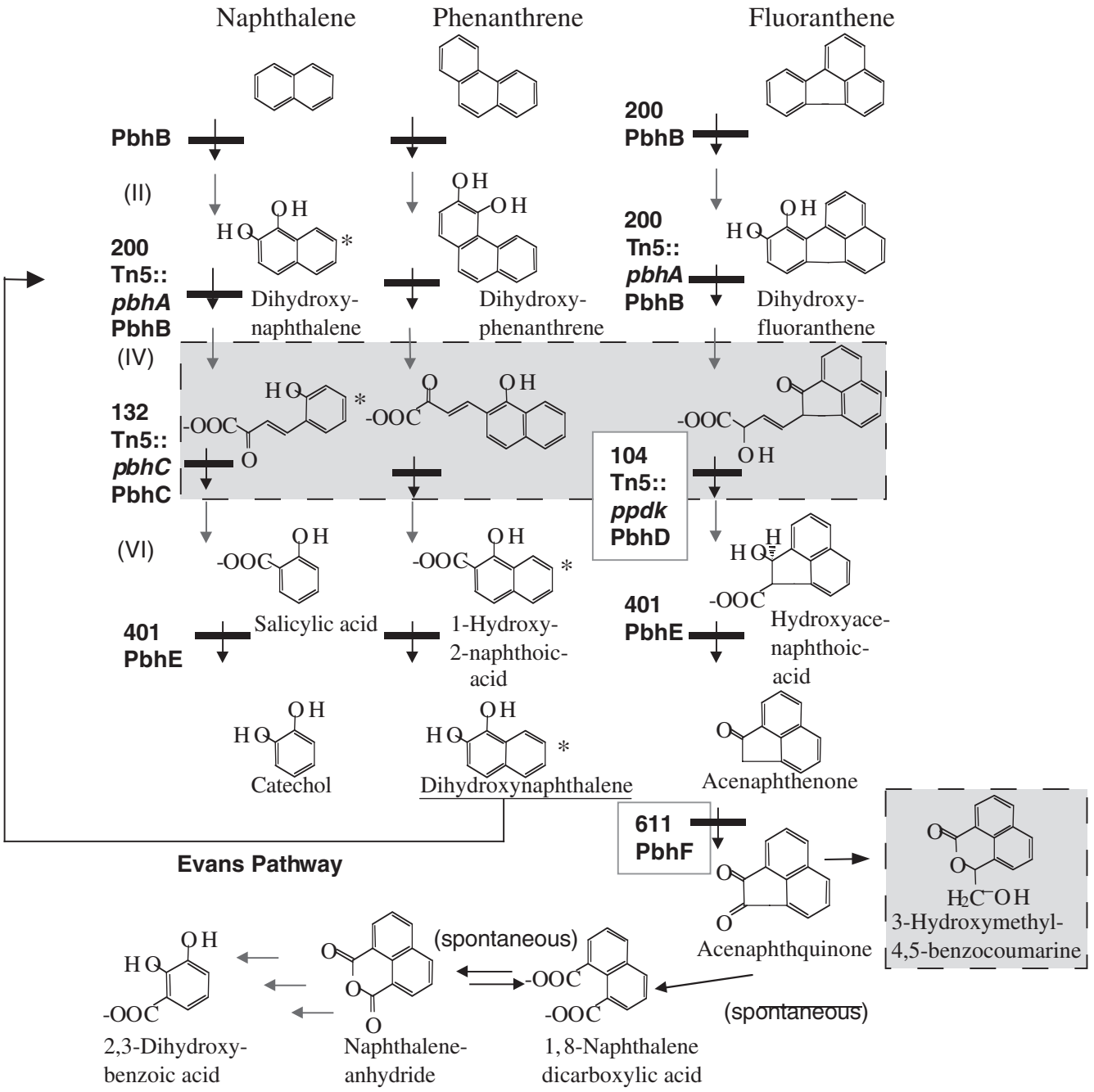

Figure 5 Proposed partial catabolic pathways for utilization of naphthalene, phenanthrene, and fluoranthene by *S. paucimobilis* EPA505. Cross bar indicates the position of the catabolic block imposed by the Tn5 insertion in mutants. Mutant phenotype is designated as 200 PbhB with lack of expression of dioxygenase genes, 401 PbhE a defect in a hydroxylase reaction, or 611 PbhF a defect in an oxygenase reaction. Mutant genotype/phenotype indicates actual location of the Tn5 insert in 200 Tn5:*pbhA* PbhB within a *meta* ring fission dioxygenase and probable polar effect on that encoding for PbhB, 132 Tn5:*pbhC* PbhC with direct disruption of expression of an aldolase hydratase PbhC, and 104 Tn5:*ppdk* PbhD Tn5 insertion within a pyruvate phosphate dikinase gene with hypothesized polar effect on expression of a fluoranthene-specific aldolase hydratase PbhD. All compounds shown were detected with the wild type and/or mutants. Shaded compounds are hypothesized based on HPLC and GC-MS analyses and other compounds detected matched that of the standards used. Mutants 104 Tn5:*ppdk* PbhD and 611 PbhF enclosed by squares indicate a divergence in further catabolism of fluoranthene from naphthalene and phenanthrene. Roman numerals indicate other enzymes and their respective substrates that are inferred in the pathways based on previous studies: (II) dehydrogenase/dihydrodiols, (IV) isomerase/*cis* isomers of open ring compounds, (VI) dehydrogenase/hydroxy aromatic aldehydes. More than one arrow indicates further catabolism by more than one enzyme.

GC-MS analysis of extracts of FLA-grown wild type EPA505 revealed the transient appearance of five compounds over 72 h incubation (Table 3). These were identified as dihydroxyfluoranthene, acenaphthenone, acenaphthquinone, naphthalene anhydride, and 2,3-dihydroxy-benzoic acid. During the time course incubation, the disappearance of acenaphthenone

and acenaphthquinone was followed with an increase in the amount of naphthalene anhydride. During incubation of EPA505 with FLAd_{10}, the deuterated forms of dihydroxyfluoranthene, acenaphthenone, acenaphthquinone, and naphthalene anhydride were detected that had a similar GC retention time as the nondeuterated forms with a predicted increase in atomic mass units (Table 3).

Discussion

Disruption of dioxygenases involved in the initial catabolism of PAHs

Three classes of Tn5 mutants of *S. paucimobilis* EPA505 defective in PAH degradation were used to delineate the catabolic pathways of naphthalene (NAP), anthracene (ANT), phenanthrene (PHE), or fluoranthene (FLA) utilization. The Tn5 insertion in a *meta* ring fission dioxygenase of class I mutant 200Tn5:*pbhA* resulted in a loss of the ability to catalyze dioxygenation of NAP, ANT, PHE, and FLA. Three other class I mutants (2, 300, and 394) appeared to have this same defect (Figure 5). These class I mutants did not transform indole to indigo that indicated loss of a dihydroxylating dioxygenase function [31]. In the class I mutant 200Tn5:*pbhA*, the Tn5 resides within a *meta* ring cleavage dioxygenase (*pbhA*) [31] that is generally the third enzymatic step involved in the initial catabolism of the aromatic ring component of a PAH. A gene encoding for a ferredoxin subunit component of a hydroxylating dioxygenase, *pbhB*, the first enzyme required in the catabolism of a PAH, was found directly downstream of the *meta* ring cleavage dioxygenase gene *pbhA*. The Tn5 promoter probe in this mutant (Tn5Km*tc*$^{p-}$) was in the proper orientation with the promoter controlling expression of *pbhA* and *pbhB* [31] to allow expression of the promoter reporter gene. This promoter was responsive to PAHs and intermediate catabolites [31] like other upper pathway operon of naphthalene-utilizing psuedomonads [29]. Mutant 200Tn5:*pbhA* does not produce any PAH degradation products and also cannot degrade lower pathway intermediates (salicylic acid, catechol, 1-hydroxy-2-naphthoic acid; Table 1). The wild type catalyzes *meta* fission of catechol (data not shown). Class I mutants 2 and 300, class II mutant 132Tn5:*pbhC*, and all class III mutants grow on catechol (Table 1) and have 2,3-catechol dioxygenase activity and the *ortho* fission product was not detectable. These observations indicate the Tn5 in mutant 200Tn5:*pbhA* caused a polar mutation that disrupted the expression of *pbhB* and possibly other dioxygenase genes that may be present on this operon that may be involved in both upper and lower catabolic pathways. The observation, that class I mutants 2 and 300 do not catalyze oxygenation of any of the PAHs tested but are able to utilize catechol [31] initiated by a 2,3-catechol dioxygenase, does not help to differentiate whether the Tn5 insertion in these mutants resides in a different location within the same operon where *pbhA* and *pbhB* reside or whether the Tn5 resides on another operon that harbors genes for catechol utilization. Possibly, the Tn5 insertion in mutants 2 and 300 resides downstream of *pbhA* where expression of *meta* fission dioxygenase component(s) is not affected but a dihydroxylating dioxygenase component that is disrupted. Sequence analysis of regions flanking the Tn5 in these mutants may help resolve the nature of this catabolic block.

Divergence point in fluoranthene catabolism from that of naphthalene, anthracene, and phenanthrene

The ring fission products that accumulated with class II mutant 132Tn5:*pbhC* and class III mutant 104Tn5:*ppdk* were possibly derived from the same *meta* ring fission dioxygenase disrupted in the class I mutant 200Tn5:*pbhA* (Figure 5). The Tn5 promoter probe in 132Tn5:*pbhC* inserted within an aldolase hydratase that is specific for NAP, ANT, and PHE degradation and does not affect FLA degradation [31], and a promoter region was found directly upstream of the aldolase hydratase gene. In contrast, a different gene is disrupted in 104Tn5:*pbhD* that prevents its growth on FLA but does not affect growth on NAP, ANT and PHE. These observations demonstrate that subsequent step(s) for FLA catabolism diverges from that of the NAP, ANT, and PHE catabolic pathway at the point of the hydratase aldolase reaction, indicating there are at least two distinct functional aldolase hydratase enzymes involved; one for FLA and another for NAP, ANT, and PHE (Figure 5).

Class III mutants 5, 104Tn5:*ppdk*, and 723 accumulated a ring fission product of FLA whose structure is proposed in Figure 4A, and small amounts of intermediate catabolites that occur later in the pathway including acenaphthenone, acenaphthquinone, and naphthalene anhydride were detected (Table 3). Some possibilities may account for the appearance of the latter catabolites including (1) an altered function or expression of a FLA-specific aldolase hydratase that was partially active, (2) low specificity of the NAP, ANT, and PHE aldolase hydratase acting at the FLA ring fission catabolite, or (3) altered regulatory function, or (4) altered cellular uptake of a FLA-derived catabolite. Class III mutant 104Tn5:*ppdk* contained the Tn5 element within a region that shares homology with the pyruvate phosphate dikinase gene [31]. In *S. aromaticivorans* F199, a *ppdk* gene has been found in an operon involved in catabolism of aromatic compounds [26]. However, the involvement of PPDK in metabolism of aromatic compounds has not been determined. PPDK is involved in the uptake of glucose in plant and bacterial cells by a group translocation mechanism [23]. It maybe possible that PPDK performs a similar function in cellular uptake of a fluoranthene-derived catabolite across the membrane in strain EPA505 although there is no evidence that this occurs. It is more likely that a Tn5 disruption of *ppdk* caused a polar mutation affecting the expression of a FLA-specific gene downstream the Tn5 insertion site and we propose that the Tn5 insertion has affected expression of another aldolase hydratase gene and this mutant phenotype is designated PbhD.

Common hydroxylase involved in naphthalene, anthracene, phenanthrene, and fluoranthene catabolism

Class I mutant 401PbhE is unable to utilize NAP, ANT, PHE, and FLA as sole carbon sources because it accumulated salicylic acid, 1-hydroxy-2-naphthoic acid, 2-hydroxy-3-naphthoic acid, and hydroxyacenaphthoic acid, when incubated with NAP, PHE, ANT, and FLA, respectively (Table 2). This observation reveals another convergence point in the NAP, ANT, PHE, and FLA catabolic pathways (Figure 5) and indicates that the Tn5 insertion disrupted the expression of a hydroxylase or dioxygenase (the Evans or Kiyohara pathways, respectively) [6,21]. If at this point in the PAH catabolic pathway a dioxygenase is

involved, then the ring fission product carboxylatophenyl-oxobutenoate would be expected from ring fission of 1-hydroxy-2-naphthoic acid (1,2-HNA) [21]. This catabolite was identified in a previous study produced by a *Nocardioides* sp. growing on phenanthrene [1]. Alternatively, if a hydroxylase is involved at this point in the pathway, then 1,2-HNA would be converted to the dihydroxynaphthalene that would then be shuttled to the upper catabolic pathway for naphthalene degradation and dihydroxynaphthalene would be cleaved by *ortho* or *meta* fission to produce a ring fission product [6]. Mutant 401PbhE does not utilize salicylic acid but can grow on catechol as a sole carbon source and mutant 132Tn5:*pbhC* can utilize both salicylic acid and catechol as a sole carbon source. When mutant 132Tn5:*pbhC* was incubated with 1,2-HNA, it accumulated a compound that we propose to be *trans-o*-hydroxybenzylidene pyruvate. A similar mass spectrum was given by Eaton [8] for the NAP ring fission product using trimethylsilyl-derivatizing reagent. Additionally, the UV absorption spectrum of this NAP-derived catabolite (Figure 1B) is identical to that of *trans-o*-hydroxybenzylidene pyruvate from NAP metabolism by a *Pseudomonas* sp. [9] and similar to the compound that accumulated with a knockout mutant of *S. yanoikuyae* B1 disrupted in an isomerase gene during incubation with NAP [20]. Mutant 132Tn5:*pbhC*, which lacks aldolase hydratase activity, was expected to accumulate this NAP ring fission product during incubation with 1,2-HNA if it retained hydroxylase activity.

Biochemical evidence suggests more than one operon is involved in aromatic catabolism

The dioxygenase genes *pbhA* and *pbhB* involved in the initial catabolism of NAP, ANT, PHE, and FLA are most likely localized in an operon separate from *pbhC* and *ppdk* and other genes involved in subsequent metabolic reactions that we infer from mutant phenotypes represented as PbhD, PbhE, and PbhF. The well-studied NAH7 plasmid in *Pseudomonas* species carries inducible genes for NAP utilization that are organized in clusters within upper and lower pathway operons (*nah* and *sal*) [29]. The *nah* operon contains genes that transform NAP to salicylic acid (SAL). SAL is further catabolized by enzymes encoded by the *sal* operon. Both operons are controlled by NahR that is part of the family of LysR transcriptional activators [29]. A promoter region directly upstream of the disrupted aldolase hydratase gene in mutant 132Tn5:*pbhC* was found that has a binding site for a LysR transcriptional activator [31]. The hydroxylase-negative phenotype of mutant 401PbhE indicates that genes involved in further metabolism of hydroxyaromatic acids are not on the same operon as the aldolase hydratase gene disrupted in 132Tn5:*pbhC*. Two observations support this hypothesis; (1) mutant 401 does not grow on fluoranthene while 132Tn5:*pbhC* does and (2) 132Tn5:*pbhC* has hydroxylase activity as observed by its ability to transform HNA to the open ring fission product of NAP that must have derived from the previous intermediate, dihydroxynaphthalene (Figure 5). The accumulation of hydroxyaromatic acids of during incubation of 401PbhE with NAP, ANT, PHE, or FLA may indicate (1) the presence of a separate lower pathway operon that encodes a hydroxylase and possibly other enzymes for further metabolism of lower pathway PAH intermediates; (2) the hydroxylase gene resides downstream of the *meta* ring fission dioxygenase disrupted in mutant 200Tn5:*pbhA*; or (3) the hydroxylase gene resides downstream of a fluoranthene-specific gene that is disrupted in mutant 104Tn5:*ppdk*. Since both mutants 132Tn5:*pbhC* and 401PbhE grow on catechol, it is proposed that genes for catechol metabolism also reside on a separate operon than the aldolase hydratase disrupted in 132Tn5:*pbhC* and the hydroxylase gene disrupted in 401PbhE. Alternatively, the catechol-degradative genes may reside upstream of the hydroxylase gene. Further analysis of nucleotide sequences is needed to understand the structure of these catabolic operons.

Another divergence point in the fluoranthene catabolic pathway from naphthalene, anthracene, and phenanthrene

The catabolic pathway for FLA utilization again diverges from that of NAP, ANT, and PHE at some point beyond the hydroxylase reaction acting on the hydroxyaromatic acid degradation products of NAP, ANT, PHE, and FLA. We presume that this is because of the difference in the chemical structure of the FLA catabolic intermediates (Figure 5). This proposal is supported by the observation that the Tn5 insertion resulted in mutant phenotypes (designated PbhD and PbhF) that inhibit utilization of FLA but do not affect the utilization of NAP, ANT, and PHE. The metabolic pathway of FLA utilization has not been well defined due to limited information on microbial degradation of PAHs containing a cyclopentane moiety. Mueller *et al.* [22] proposed three possible pathways for the initial attack on FLA involving dioxygenation and *meta* ring fission. Previous reports on FLA degradation by *Mycobacterium* PYR-1 demonstrate *meta* fission followed by the formation of the intermediate catabolite fluorenone carboxylic acid [19]. We detected small amounts of fluorenone carboxylic acid with the wild type EPA505, but not with its mutants. Weissenfels *et al.* [32] identified acenaphthenone and hydroxymethyl benzylcoumarine (HMBC) during FLA degradation by *A. denitrificans* WWI and indicated the removal of the aldehyde group from hydroxyacenaphthaldehyde to yield acenaphthenone. In our study, the identification of hydroxyacenaphthoic acid that accumulated with mutant 401PbhE suggests that a dehydrogenase, and possibly a decarboxylase, is involved to yield acenaphthenone that accumulated with mutant 611PbhF. Alternatively, an unusual hydroxylase reaction that removes the carboxyl group without subsequent hydroxylation may lead to acenaphthenone or acenaphthenol (Figure 5). The observation that EPA505 converts fluorene to hydroxyindane and indanone (Table 3) supports the hypothesis of a one-carbon excision step. Interestingly, strain EPA505 does not grow on fluorene and appears to accumulate a number of catabolic intermediates (data not given).

The detection of acenaphthquinone in culture supernating with the wild type EPA505 growing on FLA indicates that acenaphthenone is acted on by a monooxygenase reaction that is not present in mutant 611PbhF (Figure 5). A possible mode of attack on the cyclopentane of acenaphthenone may involve the incorporation of one oxygen atom of dioxygen into the cyclopentane moiety similar to that observed during microbial degradation of camphor and cyclohexanol [5,7]. In our study and another [28], a spontaneous oxidation of acenaphthquinone would then yield 1,8-naphthalene-dicarboxylic acid.

Hydroxymethylbenzocoumarine (HMBC) was identified by nuclear magnetic spectroscopy from cultures of *A. denitrificans*

WW1 grown with FLA [32]. HMBC is thermally unstable and not amenable to GC-MS analysis. We used a similar HPLC method as Weissenfels *et al.* and found a compound with the same UV absorption spectrum and similar HPLC retention time as HMBC when EPA505 or mutant 611PbhF was incubated with FLA (Figure 1N). This compound was found in the acidified extraction fraction that was brown at pH 2 and black at pH 7. When this compound was purified and concentrated by HPLC and derivatized with TMS for gas chromatographic analysis, no compounds were detected. NMR analysis may reveal the identity of this compound that coincides with the appearance of acenaphthenone when mutant 611PbhF is incubated with fluoranthene.

FLA catabolic intermediates detected with the wild type included dihydroxyfluoranthene and its proposed *meta* ring fission product, acenaphthenone, acenaphthquinone, naphthalene anhydride, and 2,3-dihydroxybenzoic acid (Figure 5). Selifonov *et al.* [30], investigating the bacterial transformation off acenaphthene and acenaphthylene, identified acenaphthenone, acenapthquinone, and naphthalene anhydride. Naphthalene anhydride is thought to result from spontaneous oxidation of acenaphthquinone, yielding 1,8-naphthalene-dicarboxylic acid (1,8-NDA) that is dehydrated following solvent extraction at acidic pH.

This is the first report of the biochemical characterization of intermediate catabolites accumulated by Tn5 insertion mutants of *S. paucimobilis* EPA505 defective in PAH degradation. Further analysis of cloned fragments from plasmid DNA from Tn5 mutants will provide insight into other catabolic genes involved and their mode of regulation. Genetic, metabolic, and physiologic characterizations of *Sphingomonas* spp. aid our understanding of the unique biodegradative processes and the many factors involved in bacterial degradation of PAHs.

Acknowledgements

We thank Terri Gibeau of the Chemistry Department at Clemson University in helping with direct probe mass spectral analysis. This work was supported by a NSF EPSCoR doctoral research fellowship.

References

1 Adachi K, T Sano, H Iwabuchi and S Harayama. 1999. Structure of the ring cleavage product of 1-hydroxy-2-naphthoate. An intermediate of the phenanthrene-degradative pathway of *Nocardioides* sp. strain KP7. *J Bacteriol* 181: 757–763.
2 Barnsley EA. 1975. The degradation of fluoranthene and benzo[*a*]pyrene. *Can J Microbiol* 21: 1004–1008.
3 Barnsley EA. 1976. Role and regulation of the *ortho* and *meta* pathways of catechol metabolism in pseudomonads metabolizing naphthalene and salicylate. *J Bacteriol* 125: 404–408.
4 Cerniglia CE. 1984. Microbial metabolism of polycyclic aromatic hydrocarbons. *Adv Appl Microbiol* 30: 31–71.
5 Conrad HE, R DuBus and IC Gunsalus. 1961. An enzyme system for cyclic ketone lactonization. *Biochem Biophys Res Commun* 6: 293–297.
6 Davies JI and WC Evans. 1964. Oxidative metabolism of naphthalene by soil pseudomonads. *Biochem J* 91: 251–261.
7 Donoghue NA, DB Norris and PW Trudgill. 1976. The purification and properties of cyclohexanone oxygenase from *Nocardia globerula* CL 1 and *Acinetobacter* NCIB 9871. *Eur J Biochem* 63: 175–192.
8 Eaton RW. 2000. *Trans-o*-hydroxybenzylidene pyruvate aldolase hydratase as a biocatalyst. *Appl Environ Microbiol* 66: 2668–2672.
9 Eaton RW and PJ Chapman. 1992. Bacterial metabolism of naphthalene: construction and use of recombinant bacteria to study the ring cleavage of 1,2-dihydroxynaphthalene and subsequent reactions. *J Bacteriol* 174: 7542–7554.
10 Feiser LF and J Cason. 1940. *O*-Halide synthesis of 10-methyl-1,9-methylene-1,2-benzanthracene. *J Am Chem Soc* 62: 432–436.
11 Fredrickson JK, FJ Workman, DJ Brockman, SW Li and TO Stevens. 1991. Isolation and characterization of a subsurface bacterium capable of growth on toluene, naphthalene and other aromatic compounds. *Appl Environ Microbiol* 57: 796–803.
12 Grund AD and IC Gunsalus. 1983. Cloning of genes for naphthalene metabolism in *Pseudomonas putida*. *J Bacteriol* 156: 89–94.
13 Haigler BE, GR Johnson, W-C Suen, and JC Spain. 1999. Biochemical and genetic evidence for *meta*-ring cleavage of 2,4,5-trihydroxytoluene in *Burkholderia* sp. strain DNT. *J Bacteriol* 181: 965–972.
14 Heitkamp MA, JP Freeman, DW Miller and CE Cerniglia. 1988. Pyrene degradation by a *Mycobacterium* sp.: identification of ring fission products. *Appl Environ Microbiol* 54: 2556–2565.
15 Jackson MM, Y Yang and PH Pritchard. 1999. Metabolism of fluoranthene by *Sphingomonas paucimobilis* sp. strain CO6 and its proposed pathway. Abstracts of the American Society for Microbiology 99th Meeting, p. 580.
16 Jerina DM, PJ Van Balderen, H Yagi, DT Gibson, V Mahadevan, AS Neese, M Koreeda, ND Sharma and DR Boyd. 1984. Synthesis and absolute configuration of the bacterial *cis*- 1,2 and *cis*- 10,11 dihydrodiol metabolites of benz[*a*]anthracene formed by a strain of *Beijerinkia*. *J Org Chem* 49: 3621–3628.
17 Kanaly I and S Harayama. 2000. Biodegradation of high molecular weight polycyclic aromatic hydrocarbons by bacteria. *J Bacteriol* 182: 2059–2067.
18 Kelley I and CE Cerniglia. 1991. Metabolism of fluoranthene by a species of *Mycobacterium*. *J Ind Microbiol* 7: 19–26.
19 Kelley I, JP Freeman, FE Evans and CE Cerniglia. 1991. Identification of a carboxylic acid metabolite from the catabolism of fluoranthene by a *Mycobacterium* sp. *Appl Environ Microbiol* 57: 636–641.
20 Kim E and GJ Zylstra. 1999. Functional analysis of genes involved in biphenyl, naphthalene, phenanthrene and *m*-xylene degradation by *Sphingomonas yanoikuyae* B1. *J Ind Microbiol Biotechnol* 23: 294–302.
21 Kiyohara H, K Nagao and R Nami. 1976. Degradation of phenanthrene through *o*-phthalate by *Aeromonas* sp. *Agric Biol Chem* 40: 1075–1082.
22 Mueller JG, PJ Chapman, BO Blattmann and PH Pritchard. 1990. Isolation and characterization of a fluoranthene-utilizing strain of *Pseudomonas paucimobilis*. *Appl Environ Microbiol* 56: 1079–1086.
23 Pocalyko DJ, LJ Carrol, BM Martin, PC Babbit and D Dunaway-Mariano. 1990. Analysis of sequence homologies in plant and bacterial pyruvate phosphate dikinase, enzyme 1 of the bacterial phosphoenolpyruvate, sugar phosphotransferase system and other PEP-utilizing enzymes: identification of potential catalytic and regulatory motifs. *Biochemistry* 29: 10757–10765.
24 Pothuluri JV, JP Freeman, FE Evans and CE Cerniglia. 1990. Fungal transformation of fluoranthene. *Appl Environ Microbiol* 56: 2974–2983.
25 Resnick SM and DT Gibson. 1996. Regio- and sterospecific oxidation of fluorene, dibenzofuran and dibenzothiophene by naphthalene dioxygenase from *Pseudomonas* sp. strain NCIB 9816-4. *Appl Environ Microbiol* 62: 4073–4080.
26 Romine MF, LC Stillwell, K-K Wong, SJ Thurston, EC Sisk, C Sensen, T Gaasterland, JK Fredrickson and JD Saffer. 1999. Complete sequence of a 184-kilobase catabolic plasmid from *Sphingomonas aromaticavorans* F199. *J Bacteriol* 181: 1585–1602.
27 Romine MF, JK Fredrickson and S-MW Li. 1999. Induction of aromatic catabolic activity in *Sphingomonas aromaticavorans* strain F199. *J Ind Microbiol Biotechnol* 23: 303–313.
28 Sepic E, M Bricelj and H Leskovsek. 1997. Biodegradation of polyaromatic hydrocarbons in aqueous media. *J Appl Microbiol* 83: 561–568.

29 Schell MA. 1993. Molecular biology of the LysR family of transcriptional regulators. *Annu Rev Microbiol* 47: 597–626.
30 Selifonov SA, M Grifoll, RW Eaton and PJ Chapman. 1996. Oxidation of naphthenoaromatic and methyl-substituted aromatic compounds by naphthalene 1,2-dioxygenase. *Appl Environ Microbiol* 62: 507–514.
31 Story SP, SH Parker, JD Kline, T-RJ Tzeng, JG Mueller and EL Kline. 2000. Identification of four structural genes and two putative promoters necessary for the utilization of naphthalene, phenanthrene and fluoranthene by *Sphingomonas paucimobilis* var. EPA505. *Gene* 260: 155–169.
32 Weissenfels WD, M Beyer, J Klein and HJ Rehm. 1991. Microbial metabolism of fluoranthene: isolation and identification of ring fission products. *Appl Microbiol Biotechnol* 34: 528–535.
33 Zink G and KE Lorber. 1995. Mass spectral identification of metabolites formed by microbial degradation of polycyclic aromatic hydrocarbons (PAH). *Chemosphere* 31: 4077–4084.